Available online at www.garmian.edu.krd

Passer Journal of Basic and Applied Sciences

Passer 7(Issue 1) (2025) 442-451

Original Article

Impact of Eyring-Powell Fluid Flow with MHD and Gyrotactic Microorganisms on a Permeable Stretching Sheet

P. Madhu Sravanthi[1], M. Radha Madhavi*[2]

[1]*Research Scholar, Department of Mathematics, Koneru Lakshmaiah Education Foundation, Guntur, AP, 522502, India.*
[2]*Department of Mathematics, Koneru Lakshmaiah Education Foundation, Guntur, AP, 522502, India.*

Received 11 June 2024; revised 17 August 2024;
accepted 25 August 2024; available online 18 June 2025

DOI: 10.24271/PSR.2024.462397.1627

ABSTRACT

This article's main aim is to explore the impact of Eyring-Powell fluid flow on gyrotactic microorganisms over a stretched sheet, considering the incidence of chemical reactions and porous media. By employing the similarity variable technique, the PDEs are converted into ODEs. The variations in velocity, high temperature, concentration, and motility distributions are exemplified through graphical representations. These results are achieved using the Runge-Kutta-Fehlberg method with a shooting strategy implemented in MATLAB. Numerical values for the Sherwood number, the skin friction coefficient, the motile density number, and the Nusselt number are presented in tabular form. The study provides a comprehensive analysis of the interaction between fluid dynamics and microorganism behavior. Additionally, it offers insights into optimizing industrial and biomedical applications involving such complex fluid flows.

Keywords: Brownian motion, Prandtl number, Schmidt number, Magnetic field and Motility distributions.

1 Introduction

A nanofluid that consists of nano-sized particles recognized as nanoparticles. Nanoparticles are often utilized in nanofluids composed of metals, carbides, and oxides. Microorganisms that can be visible only under the microscope. Microorganisms are helpful in food production, wastewater treatment, biofuel production, and constructing a wide range of chemicals and enzymes. Microorganisms are employed in fermentation to produce yogurt, cheese, curd, and other foods. Fermentation microorganisms add flavor and aromas. Vitamins C, B2, and B12 are produced by microorganisms. Microorganisms, with a few exceptions, are utilized to produce medicines such as penicillin and tetracycline. The influence of thermal conductivity in different materials and flow in the boundary layer over a stretched sheet must be studied due to their significant applications in various biological processes, production procedures, and industrial structures such as paper processing, bubble absorption, metal extrusion, and fermentation. These applications are referenced in [1-6]. Khan, M [7], aimed to investigate the effects of variable viscosity on Williamson nanofluid over a non-linear stretching sheet. D. A. Neild *et al.* [8] investigated the stability analysis to explore the onset of bioconvection in a horizontally layered suspension-containing fluid of motile microbes with heating or cooling from below. W. N. Mutuku *et al.* [9] studied the bioconvection caused by the hydromagnetic flow of a special type of nanofluid based on water containing nanoparticles and motile bacteria over a permeable vertically moving surface.

* Corresponding author
E-mail address mrmadhavi5@gmail.com (Instructor).
Peer-reviewed under the responsibility of the University of Garmian.

T M. Waqas *et al.* [10] invented magneto hydrodynamic moving nanomaterials in a medium characterized by layers with gyrotactic microbes. This investigation focuses on MHD stalemate Powell-Eyring nanofluid flow with bifurcation by M. Ramzan. *et al.* [11]. In the current study, using an artificial neural network, the slip and Darcy-Forchheimer procedure was investigated for bioconvective applications of the stretched Powell-Eyring nanofluid model. This is discussed by Andac Batur Colak *et al.* [12] and F. Naseem *et al.* [13]. The current study focuses on the behavioural properties of gyrotactic microbes to define their function in heat & mass transport in Powell-Eyring nanofluids if MHD forces are present. A.O. Alharbi. *et al.* [14] briefly explores the impact of entropy caused by magnetohydrodynamic Eyring-Powell fluid on an unstable oscillating porous stretched sheet. M. Bilal [15] and others conducted this study to investigate heat exchange in the presence of Eyring-Powell fluid convective flow across a layered stretched sheet. The fluid is viscous, incompressible, two-dimensional, and laminar in nature.

T. Hayat *et al.* [16] explained the heat exchanger of an Eyring Powell fluid across a constantly moving plane is investigated when there is a free stream velocity. A.A. Bossly *et al*. [17]. This study will look at the constant, Eyring-Powell fluid containing gyrotactic microorganisms that flow laminar and incompressible via a layered stretching surface. M. Radha Madhavi *et al*. [18-19]. The goal of the article is to look at the source of heat across a wedge via porous media for the flow of fluid that conducts electricity in a magnetohydrodynamic system. The flow of radiative and incompressible Jeffrey fluid along porous media across a starching sheet is illustrated using magnetohydrodynamics. C. Srinivas Reddy *et al*. [20] proposed to explore the behavior of gyrotactic microorganisms to demonstrate the importance of heat & mass transfer in an MHD unstable Eyring-Powell nanofluid flowing employing a static wedge. G.R. Ganesh, W. Sridhar *et al*. [21] discussed Entropy exploration, higher order nanofluid flow chemical reaction of Casson, and MHD and electric field impacts are all topics of the current investigation G. Dharmaiah, W. Sridhar *et al.* [22] investigates radiation impact, diffusion, and iron slip on a nano liquid magneto-titanium alloy. W. Sridhar *et al.* [23] established the relationship between fluid flow sheets and mathematical modelling of magnetic fields, porous media, heat propagation, and heat transfer by radiation for constant and variable thickness. N. Vijaya *et al.* [24] are studied to investigate the advancements in Casson fluid that conducts electricity generated by a porous elongated surface while accounting for Arrhenius energy of activation, viscosity dissipation, and joule heating. N. Vijaya *et al*. [25] study seeks to invent the qualities of thermophoresis & Brownian motion-induced mass and heat transfer processes Casson Nano fluid is applied as a liquid thin coating across an extended sheet. The influence of Casson nanoparticles on thermophoretic and Brownian forces is investigated. N. Vijaya *et al*. [26] the primary goal of the investigation is to investigate Maxwell fluid in the presence of impact of buoyancy forces brought on order of magnitude extending sheet during a chemical reaction. P. Madhu Sravanthi *et al.* [27] studied the Gyrotactic microorganisms present on a stretched surface with activation energy and magnetic field, and nanofluid flow occurs. P. Madhu Sravanthi. [28] investigates impacts of thermophoresis and chemical reactivity on a Casson nanofluid's MHD wedge flow. Mardan Ameen Pirdawood *et al*. [29], introduce the Modelling impact of exposure rate to contaminated water on the spread of cholera disease through integrating sensitivity analysis and the explicit Runge-Kutta method. G Vijaya Lakshmi [30] is investigating the heat and mass transfer enhancement effect with an MHD hybrid nanofluid permeable starching sheet. Ali, H.M., and Rehman[31] studied thermal energy storage (TES) which has grown in significance due to the intermittent nature of renewable energy sources and the necessity to manage waste heat released into the environment effectively.

The current article investigates the effect of Eyring-Powell fluid with MHD flow consisting of Gyrotactic microorganisms on the stretched sheet in the existence of permeability and chemical reaction. The MATLAB software is used to estimate Skin friction, Nusselt, local density number of motile microorganisms, and Sherwood number for variations of distinct parameters.

2 Methods and Materials

The study of the inexhaustible flow of a hybrid convection Eyring-Powell fluid passing along the stretched plane. Figure 1 depicts the problem geometry. $U_w = ax$ is the stretching velocity on the x – axis and on the y - axis fluid flow is taken. u, v are nanofluid velocities where a is +ve term. Proposed model is defined as [10,15]

$$\sinh^{-1}\left(\frac{1}{\bar{c}}\frac{\partial u_i}{\partial x_j}\right) \cong \frac{1}{\bar{c}}\frac{\partial u_i}{\partial x_j} - \frac{1}{6}\left(\frac{1}{\bar{c}}\frac{\partial u_i}{\partial x_j}\right)^3, \frac{1}{\bar{c}}\frac{\partial u_i}{\partial x_j} << 1.$$

The governing equations are as below [17]

$$\frac{\partial u}{\partial x} + \frac{\partial v}{\partial y} = 0 \tag{1}$$

$$u\frac{\partial u}{\partial x} + v\frac{\partial u}{\partial y} = \left(\nu + \frac{1}{\rho_f \beta c}\right)\frac{\partial^2 u}{\partial y^2} - \frac{1}{2\rho_f \beta \bar{C}^3}\frac{\partial^2 u}{\partial y^2}\left(\frac{\partial u}{\partial y}\right)^2 - \frac{\sigma^* B_0^2}{\rho_f}u - \frac{\nu}{k}u + \frac{g}{\rho_f}[\rho_{f\infty}\beta_v(T - T_\infty) - (C - C_\infty)(\rho_p - \rho_{f\infty}) - \gamma(m - m_\infty)(\rho_{mr} - \rho_{f\infty})] \tag{2}$$

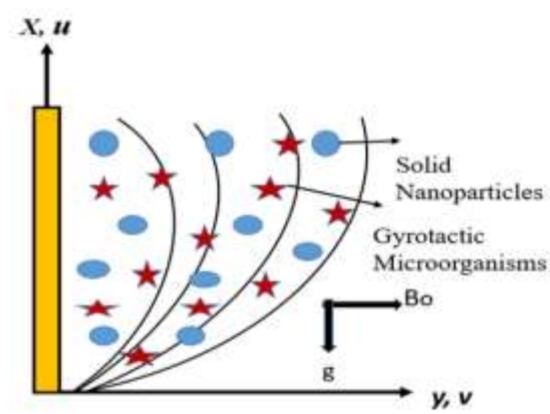

Figure 1: Problem geometry.

$$u\frac{\partial T}{\partial x} + v\frac{\partial T}{\partial y} = \frac{k}{\rho C_p}\frac{\partial^2 T}{\partial y^2} + \tau\left(\frac{D_T}{T_\infty}\left(\frac{\partial T}{\partial y}\right)^2 + D_B\frac{\partial T}{\partial y}\frac{\partial C}{\partial y}\right) + \frac{Q}{\rho C_p}(T - T_\infty) + \frac{16\sigma^* T_\infty^3}{3k^* \rho C_p}\frac{\partial^2 T}{\partial y^2} + \frac{\mu}{\rho C_p}\left(\frac{\partial u}{\partial y}\right)^2 \tag{3}$$

$$u\frac{\partial C}{\partial x} + v\frac{\partial C}{\partial y} = D_B\frac{\partial^2 C}{\partial y^2} + \frac{D_T}{T_\infty}\frac{\partial^2 T}{\partial y^2} - K_1(C - C_\infty) \tag{4}$$

$$u\frac{\partial N}{\partial x}+v\frac{\partial N}{\partial y}+\frac{bw_c}{(C_w-C_0)}\left(\frac{\partial}{\partial y}\left(N\frac{\partial C}{\partial y}\right)\right)=D_m\frac{\partial^2 N}{\partial y^2} \quad (5)$$

The components in the preceding equations are v & u are the velocity components, $\sigma^*$is electrical conductivity, magnetic field strength B_0, volume expansion coefficient B_v, g is the gravitational force, dimensional material constants β & $\bar{C}$, Density of fluid and density of microorganisms is ρ_p &ρ_{mr}, specific heat C_p, kinematic viscosity v, heat capacity τ, thermophoresis term D_T, Brownian diffusion coefficient D_B, fluid temperature T, ambient temperature T_∞, fluid concentration C, ambient concentration of nanoparticles C_∞, speed of swimming cell bW_c, diffusivity of microorganism D_m, microorganism concentration N respectively.

The boundary circumstances are defined as [17]

$$u=U_w=ax, v=0, C=C_w=C_0+d_1x,$$

$$T=T_w=T_0+b_1x, N=N_w=N_0+h_1x \text{ at } y=0,$$

$$u\to 0, C\to C_\infty=C_0+d_2x, T\to T_\infty=T_0+b_2x,$$

$$N\to N_\infty=N_0+h_2x \text{ at } y\to\infty \quad (6)$$

The similarity variables as fallows

$$\psi=\sqrt{av}xf(\eta), \eta=\sqrt{\frac{a}{v}}y, u=\frac{\partial\psi}{\partial y}, v=-\frac{\partial\psi}{\partial x},$$

$$\theta(\eta)=\frac{T-T_\infty}{T_w-T_0}, \phi(\eta)=\frac{C-C_\infty}{C_w-C_0}, G(\eta)=\frac{N-N_\infty}{N_w-N_0} \quad (7)$$

By using the equation (6) the ODEs are converted into PDEs

$$(1+\epsilon)f'''-\epsilon\,\sigma f'''f''^2+ff''-f'^2-$$

$$\left(M+\frac{1}{K_p}\right)f'+\lambda(\theta-N\phi-R_bG)=0 \quad (8)$$

$$\left(1+\frac{4}{3}Rd\right)\theta''+P_r(f\theta'-e_1f'-f'\theta+$$

$$N_t\theta'^2+N_b\theta'\phi'+\gamma\theta+Ecf''^2)=0 \quad (9)$$

$$\phi''+Sc(f\phi'-e_2f'-f'\phi)+\frac{N_t}{N_b}\theta''+K_rSc\phi=0 \quad (10)$$

$$G''+Le(fG'-e_3f'-f'G)-Pe(\phi'G'+(\Omega+G)\phi'')=0 \quad (11)$$

The boundary notations after transformed are as allows.

$$f(0)=0, f'(0)=1, f'(\infty)=0, \theta(0)=1-e_1, \theta(\infty)=0,$$

$$\phi(0)=1-e_2, \phi(\infty)=0, G(0)=1-e_3, G(\infty)=0 \quad (12)$$

Where σ & ϵ are the material factors, $e_1, e_2,$ & e_3 are thermal, mass, motile density stratification factors respectively.

2.1 Numerical Solutions

Utilizing boundary conditions, the PDEs in Equation (1) to (5) are transformed into nonlinear ODEs. By applying boundary conditions (12), the ordinary differential equations from equation (10) to equation (13) are solved using MATLAB's BVP4C solver. This method ensures precise and reliable results for the complex fluid dynamics problem. Additionally, the solver's efficiency makes it well-suited for handling the computational demands of such intricate systems.

3 Results and Discussions

This article suggests that the effect of Eyring-Powell fluid with MHD flow consists of Gyrotactic microorganisms in the existence of a stretched sheet of chemical reaction and permeable media. Physical representations are used to investigate numerical results. The equations (10 – 13) utilizing the boundary circumstance (14), the temperature, concentration, velocity profiles, motile microbe's density, and mass & heat exchanger allotments examined for different constraints, in Figure (2) - (20) and table. M=1, N=0.1, Pe=0.1, Le=1,Rd=0.4, Pr=2.5, Nt=0.1, Nb=0.5, Ec=1, ϵ=0.1, Kp=1, σ = 0.4, λ =0.1, Ω =0.1, γ =0.1, R_b=0.4, $e_1=0.5$, $Sc=0.8$, $e_2=0.5$, $Kr=0.1$, e_3=0.5.

By raising the magnetic field, the velocity profiles decrease because the magnetic field creates Lorentz forces that oppose the velocity of a nanofluid is as depicted in Figure 2. In Figure 3, the velocity profiles are escalated when the porosity parameter increases. The drag force drops as the permeability of a porous media increases, which causes the fluid's velocity profile to accelerate. The material parameter ϵ values increase the velocity profiles rise. The parameter ϵ and fluid viscosity have an opposite relationship. With an increase in, the fluid flow resistance declined as the fluid velocity increased, as is seen in Figure 4. The buoyance ratio parameter values increase the velocity profiles diminish. The profiles of temperature escalate as the radiation parameter rises. Rd denotes the proportional contribution of thermal radiation transmission to conduction heat transfer, which is shown in Figure 5. Figure 6 shows that temperature constraints decrease with increasing Pr. The Prandtl number defines the ratio of momentum to thermal diffusivity. Compared to the momentum boundary layer, the thermal boundary layer is substantially thicker. So, the Prandtl increases when the temperature drops.

Figures 7 & 13 exhibit the temperature and concentration changes. The thermophoresis phenomenon involves vast numbers of nanoparticles moving against a hot to a cold region, which results in an upgrade in fluid temperature and concentration. The thermal & solutal distributions upsurge due to Nt. At 10 and 50 °C, the convection caused by the nanoparticles then Brownian motion improves the thermal conductivity of the particles. Therefore, the Brownian motion enhances the temperature field. In contrast, a diminishment in the thickness of the solutal boundary layer is seen in high values of Brownian motion Nb in the concentration profile, as seen in Figures 8 & 14. Figure 9 demonstrates the variations in temperature profiles for the Ec parameter. Eckert number Ec Parameter rises the temperature profiles are upgrading. Ec is the ratio of kinematic energy and heat enthalpy. As a result, as the Eckert number rises, kinetic energy can be transformed into internal energy by exerting effort against viscous fluid forces. Therefore, elevating Eckert number Ec raises the fluid's temperature. Actually, as e_1 increases, the temperature gradient between surface and ambient fluids decreases, which causes a fall in fluid thermal flow. Consequently, heat distribution decreases as e_1 values increase. It is depicted in Figure 10.

The Changes in Concentration profiles for Schmidt number Sc are depicted in Figure 11. Higher Sc values slow down mass diffusions and lower fluid concentration. So concentration profiles diminish with upgrading Sc values. In Figure 12 chemical reaction parameter values increasing the Solutal boundary profiles decline. The predominant reason is that with the expansion of chemical reaction parameters, a greater number of solute molecules become engaged in the reaction, which causes a reduction in the concentration field. In Figure 15 rising e_2, the volumetric fraction between reference and surface nanoparticles decreases. Because of this, as e_2 increases, the concentration distribution decreases. Figure 16 displays the motile density pattern caused by Lewis number Le. Physically, the lower estimates of Le result in a reduction of the fluid's motile density by decreasing the diffusivity of microorganisms. Therefore, when Lewis number Le increases, the motile density distribution of the microorganism decreases.

Figure 17 shows how Peclet number Pe alters the distribution of motile density in microorganisms. Increased Pe causes a reduction in microorganism diffusions, which in turn lowers the fluid's motile density of microbes. As a result, greater values of Pe result in an improvement in the motile density distribution of the microbes. Figure 18 depicts how e_3 altered the motile density distribution of microorganisms. With increasing e_3, the concentration difference between the surface and distantce from the surface diminishes. Figure 18 illustrates the outcome of e_3 on the motile density distribution of microbes. As e_3 increases, the concentration difference between the surface and areas further from the surface diminishes. This trend indicates that higher e_3 values promote a more uniform distribution of microorganisms. Ultimately, these findings highlight the critical role of e_3 in controlling microorganism concentration gradients within the fluid.

Table 1 discusses about present article results and base paper results. It is compared to very small variations from the base paper. In this paper, Kr, Kp, Ec, Rd are considered. These parameter variations are discussed in the results and discussions. Tables 2 and 3 detail the variations in skin friction, Nusselt number, local density number of motile microorganisms, Sherwood number under various parameters. These parameters include M, Kp Є, N, Rd, Pr, Nt, Nb, Ec, Sc, Kr, Le, Pe, $e_1, e_2, \& e_3$. Table 3 presents the variations in Re_x, Nu_x, Sh_x and Nn_x for different parameters.

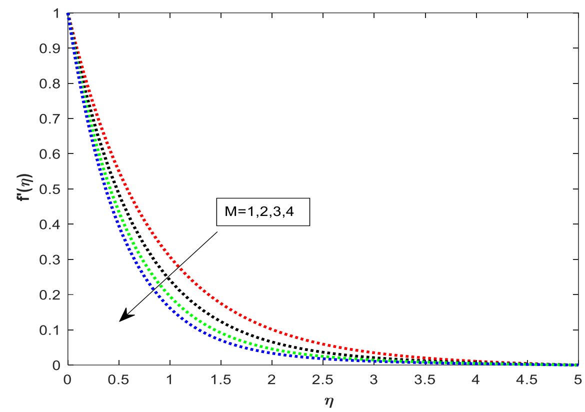

Figure 2: $f'(\eta)$ Variations of M.

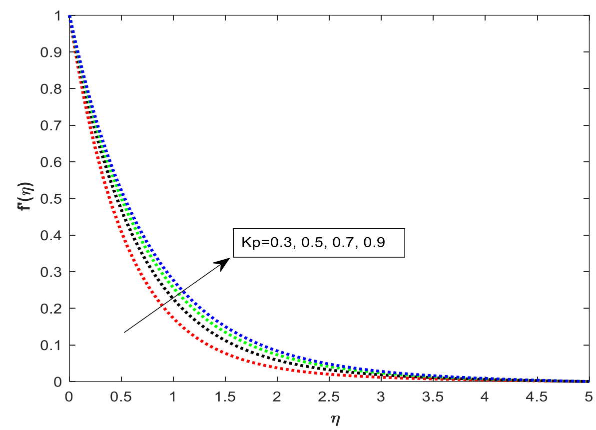

Figure 3 : $f'(\eta)$ Variations of Kp.

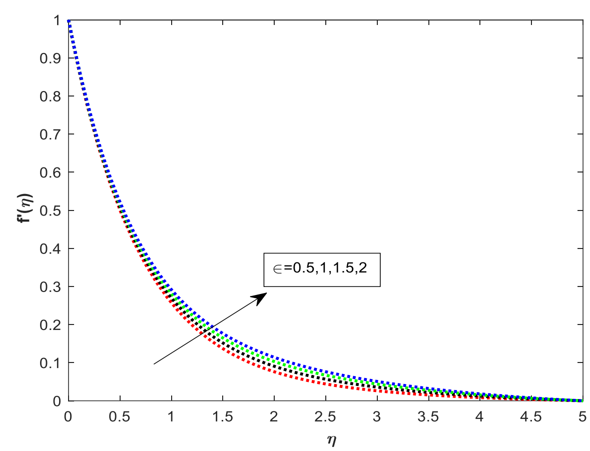

Figure 4: $f'(\eta)$ Variations of ϵ

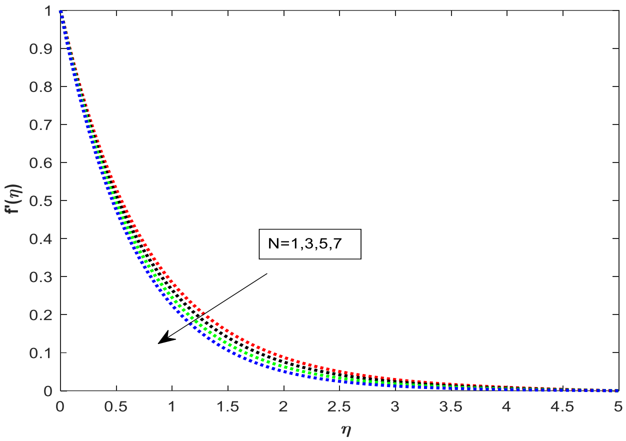

Figure 5: $f'(\eta)$ Variations of N.

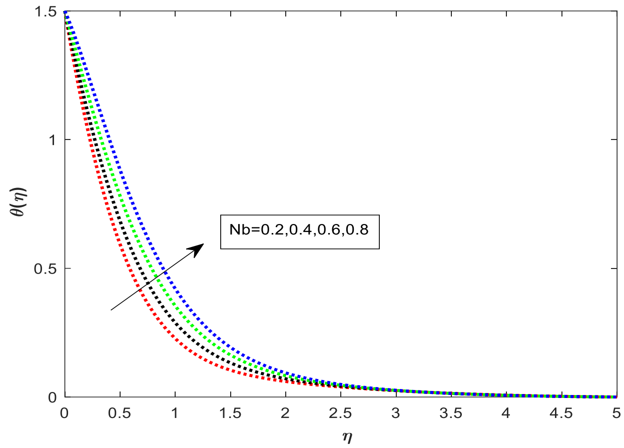

Figure 8: $\theta(\eta)$ Variations of N_b.

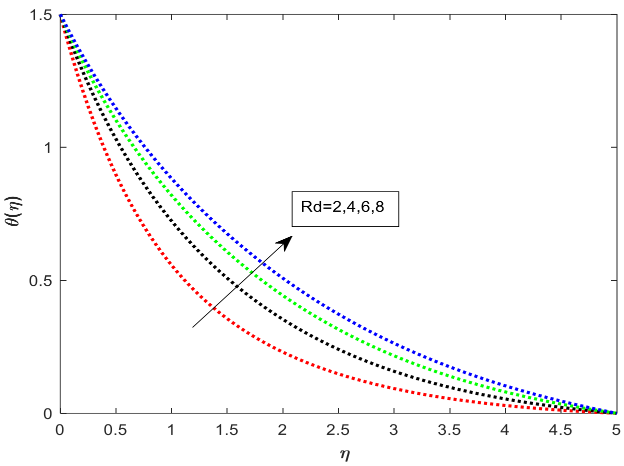

Figure 6: $\theta(\eta)$ Variations of Rd.

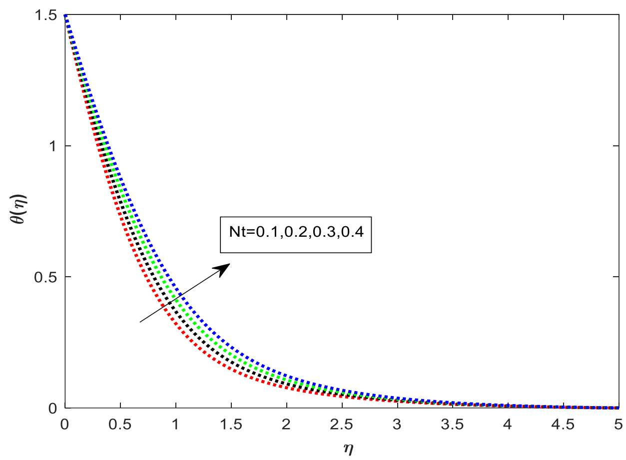

Figure 9: $\theta(\eta)$ Variations of N_t.

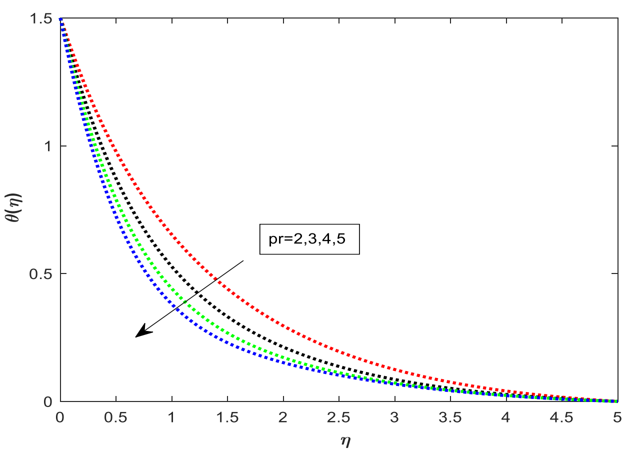

Figure 7: $\theta(\eta)$ Variations of Pr.

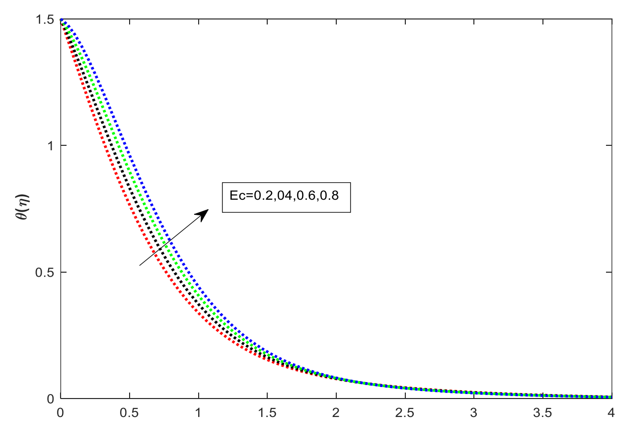

Figure 10: $\theta(\eta)$ Variations of Ec.

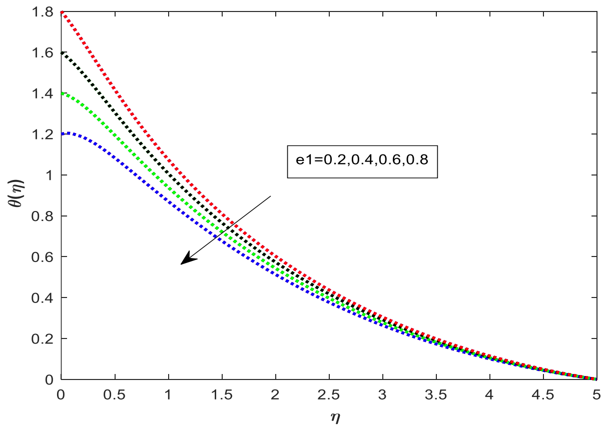

Figure 11: $\theta(\eta)$ Variations of e_1.

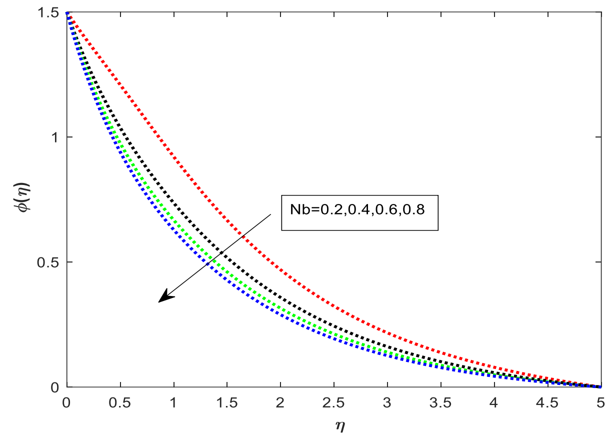

Figure 14: $\phi(\eta)$ Variations of N_b.

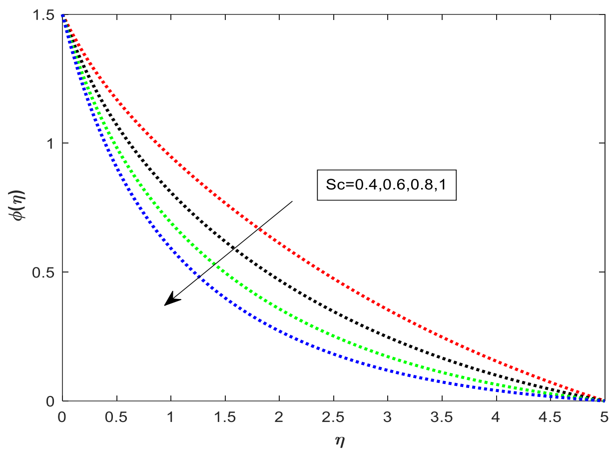

Figure 12: $\phi(\eta)$ Variations of Sc.

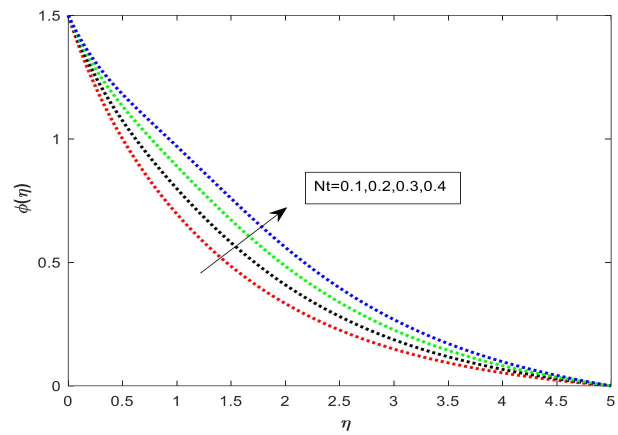

Figure 15: $\phi(\eta)$ Variations of N_t.

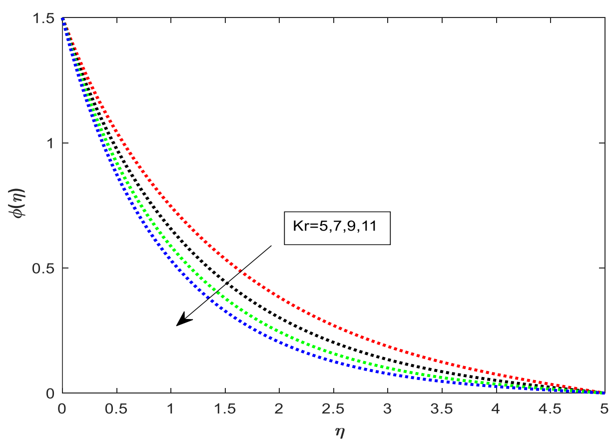

Figure 13: $\phi(\eta)$ Variations of Kr.

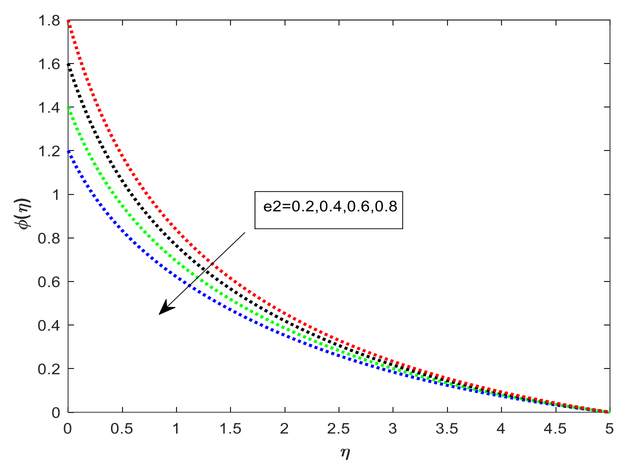

Figure 16: $\phi(\eta)$ Variations of e_2.

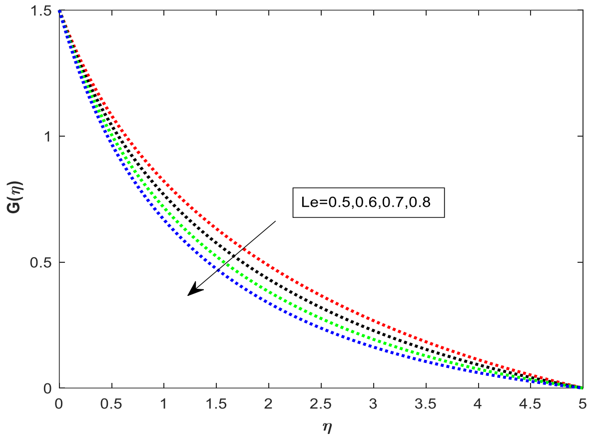

Figure 17: G(η) Variations of Le.

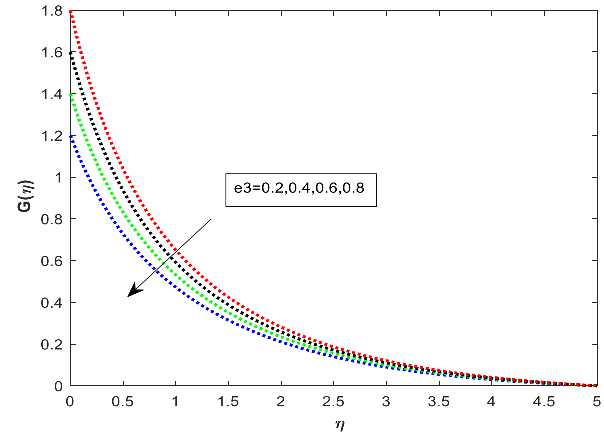

Figure 19: G(η) Variations of e_3.

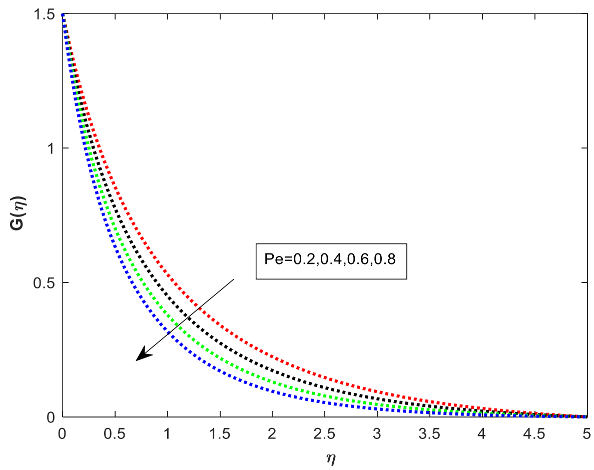

Figure 18 : G(η) Variations of Pe.

Table 1: Comparison of $-\theta'(0)$ for distinct P_r values with Kp=Rd= Ec= Kr = 0.

P_r	Afrah Al-Bossly et al. [17]	Present result
2	1.229083	1.339383
3	1.542006	1.682008
4	1.851297	1.962397
5	1.970626	2.197162

Table 2: Re_x, Nu_x, Sh_x and Nn_x variations for distinct parameters.

M	Kp	∈	N	Rd	Pr	N_b	N_t	Ec	$Re_x^{1/2}C_f$	$Nu_xRe_x^{-1/2}$	$shRe_x^{-1/2}$	$NnRe_x^{-1/2}$
1									1.213898	0.687139	1.173902	1.568339
2									1.476199	0.574617	1.178563	1.565109
3									1.704648	0.487613	1.182851	1.563917
4									1.911452	0.416811	1.186804	1.563788
	0.3								1.837642	0.441272	1.185390	1.563747
	0.5								1.547572	0.546378	1.17988	1.564597
	0.7								1.409082	0.602086	1.177335	1.565718
	0.9								1.327026	0.636899	1.175862	1.566656
		0.5							1.213898	0.687139	1.173902	1.568339
		1							1.054853	0.760909	1.171376	1.571545
		0.5							0.944527	0.815635	1.169790	1.574531
		2							0.862735	0.858163	1.168732	1.577234
			1						1.297279	0.649857	1.175338	1.567053
			3						1.362855	0.617017	1.176658	1.566070
			5						1.428981	0.582723	1.178099	1.565191
			7						1.495673	0.546913	1.179666	1.564422
				2					1.590910	1.592722	0.369204	1.583564

				4					1.551749	1.168608	0.467673	1.647469
				6					1.529417	0.958704	0.518614	1.684564
				8					1.514903	0.832299	0.550064	1.708605
					2				1.568449	1.339683	0.427272	1.619907
					3				1.598244	1.682008	0.349156	1.571976
					4				1.619463	1.962397	0.287511	1.539497
					5				1.635346	2.197162	0.237191	1.516375
						0.2			1.662241	2.537354	0.644693	1.537794
						0.4			1.636354	2.070114	1.239444	1.643395
						0.6			1.612907	1.551280	1.455049	1.692117
						0.8			1.589688	0.986315	1.575176	1.726080
							0.1		1.624545	1.816479	1.366323	1.670666
							0.2		1.615204	1.632256	1.195181	1.656298
							0.3		1.606666	1.492565	1.062742	1.647023
							0.4		1.598841	1.384265	0.954317	1.640705
								0.2	1.617337	1.600657	1.410064	1.681491
								0.4	1.603052	1.169844	1.497299	1.703007
								0.6	1.588946	0.740249	1.584186	1.724345
								0.8	1.575020	0.312014	1.670700	1.745499

Table 3: Re_x, Nu_x, Sh_x and Nn_x variations for distinct parameters.

e_1	Sc	Kr	e_2	Le	Pe	e_3	$Re_x^{1/2}C_f$	$Nu_x Re_x^{-1/2}$	$shRe_x^{-1/2}$	$NnRe_x^{-1/2}$
0.2							1.702473	0.371902	1.508285	1.698618
0.4							1.698161	0.007899	1.453175	1.692339
0.6							1.693803	0.347108	1.399784	1.686353
0.8							1.689400	0.693495	1.348041	1.680649
	0.4						1.591179	0.527031	0.882746	1.672219
	0.6						1.586495	0.435923	1.177586	1.715473
	0.8						1.582581	0.353355	1.448537	1.754904
	1						1.579311	0.278617	1.698555	1.791072
		5					1.584175	0.407536	1.185794	1.717075
		7					1.581211	0.344120	1.390912	1.746776
		9					1.578969	0.291840	1.567974	1.772289
		11					1.577191	0.247102	1.725707	1.794960
			0.2				1.696508	0.322550	1.046995	1.638947
			0.4				1.696163	0.221976	1.299664	1.672484
			0.6				1.695811	0.118773	1.553056	1.706175
			0.8				1.695451	0.012932	1.807171	1.740020
				0.5			1.701999	0.266874	1.405468	1.119863
				0.6			1.701247	0.229768	1.413234	1.239206
				0.7			1.700539	0.194059	1.420688	1.355600
				0.8			1.699874	0.159771	1.427828	1.469000
					0.2		1.695374	0.141663	1.432373	1.876861
					0.4		1.694238	0.085820	1.444091	2.262913
					0.6		1.693214	0.032938	1.455169	2.662554
					0.8		1.692292	0.017053	1.465628	3.074616
						0.2	1.695988	0.170704	1.426270	1.689310
						0.4	1.696626	0.122504	1.434872	1.833802
						0.6	1.697264	0.073946	1.443544	1.978454
						0.8	1.697901	0.025025	1.452286	2.123270

Nomenclature

u, v	components of velocity
U_w	Stretching velocity
ρ_f	Density of fluid
β , C^{-}	Dimensional constants
ρ_{mr}	Density of microorganism
M	Magnetic parameter
Le	Lewis number
D_B	Brownian diffusion
Pr	Prandtl number
Kp	Porous Parameter
Kr	Chemical reaction Parameter
ε &σ	Material parameters
N	Buoyance ratio parameter
γ	Heat generation factor
ϵ	Variable thermal conductivity constant
λ	Mixed convection
Pe	Peclet number
Sc	Schmidt number
Ec	Eckert number
N_b	Brownian motion parameter
e_1	Thermal stratification
e_2	Mass stratification factor
e_3	Motile microorganism's stratification factor
Rb	Rayleigh number
N_t	Thermophoresis parameter
Rd	Radiation parameter
N_C	Nanofluid heat capacity parameter
Ω	Difference in microorganisms concentration
T_0	Reference temperature
C_0	Reference concentration
m_0	microorganism's concentration
B_0	Magnetic field
T	Fluid temperature
T_w	Temperature of the surface
T_∞	Ambient temperature
q_w	Heat flux
β_v	Volume expansion
g	Gravitational force
$\sigma *$	Electrical conductivity
$C p$	Specific heat
D_m	Microorganisms diffusivity
m_w	Microorganisms concentration
Greek symbols	
σ	Electrical conductivity
α	Thermal diffusivity
ψ	Stream function
ν	Kinematic viscosity of the base fluid

Conclusion

The main aim of the paper is to the influence of the incompressible flow of Eyring-Powell fluid with MHD flow, which includes gyrotactic microorganisms, on the stretched sheet in the existence of permeability.

The Magnetic field M, N parameters increase the velocity profiles diminishes, for Porous term K_p, ∈ parameters it is escalates.

R_b,N_b, N_t, Ec parameters increases the temperature profiles rises. The parameters P_r, e_1 escalates temperature profiles decrease.

The parameters Schmidt number Sc, Chemical reaction parameter K_r, Brownian motion N_b, e_2 boost up the concentration profiles lessons, and the values of N_t increases concentration profiles escalate.

Lewis number Le, Peclet number Pe, e_3 parameters escalate the density of motile microorganisms' profiles declines.

Funding

Funding for the authors of this research work is not available.

Authors contribution

Both authors have jointly worked and reviewed the manuscript.

P. Madhu sravanthi: writing - original draft, Methodology, Software, Investigation, Visualization, Validation.

M. Radha Madhavi: Conceptualization, writing - reviewing and editing, Methodology, Software, Investigation, Validation.

Conflict of interests

The authors have no conflict of interest.

References

[1] Algehyne, E.A., Alhusayni, Y.Y., Tassaddiq, A., Saeed, A., Bilal, M. The study of nanofluid flow with motile microorganism and thermal slip condition across a vertical permeable surface. *Waves in Random and Complex Media*,1-18(online first), doi:10.1080/17455030.2022.2071501 (2022).

[2] Akbar, N.S., Tripathi, D., Khan, Z.H., Bég, O.A. A numerical study of magnetohydrodynamic transport of nanofluids over a vertical stretching sheet with exponential temperature-dependent viscosity and buoyancy effects. *Chem. Phys.* Lett. **661**, 20–30, doi: 10.1016/j.cplett.2016.08.043 (2016).

[3] Shafiq, A., Hammouch, Z., Sindhu, T.N. Bioconvective MHD flow of tangent hyperbolic nanofluid with Newtonian heating. *Int. J. Mech. Sci*. **133**, 759–766, doi: 10.1016/j.ijmecsci.2017.07.048 (2017).

[4] Hayat, T., Shafiq, A., Alsaedi, A., Awais, M. MHD axisymmetric flow of third grade fluid between stretching sheets with heat transfer. *Comput. Fluids*. **86**, 103–108, doi: 10.1016/j.aej.2015.03.013 (2013).

[5] Bhatti, M.M., Marin, M., Zeeshan, A., Ellahi, R., Abdelsalam, S.I. Swimming of motile gyrotactic microorganisms and nanoparticles in blood flow through anisotropically tapered arteries. *Front. Phys*. **95**, doi:10.3389/fphy.2020.00095 (2020).

[6] Ramzan, M., Bilal, M., Kanwal, S., Chung, J.D. Effects of variable thermal conductivity and non-linear thermal radiation past an Eyring Powell

nanofluid flow with chemical reaction. *Commun. Theor. Phys*. **67**, 723, doi:10.1088/0253-6102/67/6/723 (2017)

[7] Khan, M., Salahuddin, T., Malik, M.Y., Malawi. F.O. Change in viscosity of Williamson nanofluid flow due to thermal and solutal stratification. *Int. J. Heat Mass Transf*. **126**, 941–948, doi: 10.1016/j.ijheatmasstransfer.2018.05.074 (2018).

[8] Nield, D.A., Kuznetsov, A.V. The onset of bio-thermal convection in a suspension of gyrotactic microorganisms in a fluid layer oscillatory convection. *Int. J. Therm. Sci*. **45**, 990–997, doi: 10.1016/j.ijthermalsci.2006.01.007 (2006).

[9] Mutuku, W.N., Makinde, O.D., Hydromagnetic bioconvection of nanofluid over a permeable vertical plate due to gyrotactic microorganisms. *Comput. Fluids*. **95**, 88–97, doi: 10.1016/j.compfluid.2014.02.026 (2014).

[10] Waqas, M., Hayat, T., Shehzad, S.A., Alsaedi, A. Transport of magnetohydrodynamic nanomaterial in a stratified medium considering gyrotactic microorganisms. *Phys. B Condens. Matter*. **529**, 33–40, doi: 10.1016/j.physb.2017.09.128 (2018).

[11] Ramzan, M., Bilal, M., Chung, J.D. Radiative flow of Powell-Eyring magneto-nanofluid over a stretching cylinder with chemical reaction and double stratification near a stagnation point. *PLoS One*. **12**. Doi: 10.1371/journal.pone.0170790 (2017).

[12] Çolak, A.B., Shafiq, A., Sindhu, T.N. Modeling of Darcy–Forchheimer bioconvective Powell Eyring nanofluid with artificial neural network. *Chinese J. Phys*. **77**, 2435–2453, doi: 10.1016/j.cjph.2022.04.004 (2022).

[13] Naseem, F., Shafiq, A., Zhao, L., Naseem, A. MHD bioconvective flow of Powell Eyring nanofluid over stretched surface. *Aip Adv*. **7**, 65013, doi:10.1063/1.4983014 (2017).

[14] Alharbi, S.O., Dawar, A., Shah, Z., Khan, W., Idrees, M., Islam, S., Khan, I. Entropy Generation in MHD Eyring-Powell Fluid Flow over an Unsteady Oscillatory Porous Stretching Surface under the Impact of Thermal Radiation and Heat Source/Sink. *applied sciences* (n.d.), doi:10.3390/app8122588 (2018).

[15] Bilal, M., Ashbar, S. Flow and heat transfer analysis of Eyring-Powell fluid over stratified sheet with mixed convection. *J. Egypt. Math. Soc*. **28**, 1–16, doi:10.1186/s42787-020-00103-6 (2020).

[16] Hayat, T., Iqbal, Z., Qasim, M., Obaidat, S. Steady flow of an Eyring Powell fluid over a moving surface with convective boundary conditions. *Int. J. Heat Mass Transf.* **55**, 1817–1822, doi: 10.1016/j.ijheatmasstransfer.2011.10.046 (2012).

[17] Afrah Al-Bossly, Fuad S. Alduais, Showkat Ahmad Lone, Musawa Yahya Almusawa, Anwar Saeed. A stratified MHD flow of Eyring-Powell fluid containing gyrotactic microorganisms through a stretching sheet with mixed convection. *Int. J. Applied mathematics and mechanics*. **103**, 1521-4001, doi:10.1002/zamm.202200492 (2023).

[18] Radha Madhavi, M., Sridhar, W., Nagesh, P. Numerical investigations of MHD Casson nanofluid flow over a wedge through porous medium, *AIP Conference Proceedings*, **2375**, 0066944, doi:10.1063/5.0066411 (2021).

[19] Radha Madhavi, M., Veeranjaneyulu, M., Srimannarayana, N., Vijaya, N., "Impacts of thermophoresis, joule heating and soret & dufour effects on mixed convective jeffery fluid flow over an elongated sheet, *International Journal of Advanced Science and Technology*, **29**(5), 3060–3069 (2020).

[20] C.Srinivas Reddy, Farhan Ali, Khaled Al-Farhany, W. Sridhar, Numerical analysis of gyrotactic microorganisms in MHD radiative Eyring–Powell nanofluid across a static/moving wedge with Soret and Dufour effects, *ZAMM Journal of Applied Mathematics and Mechanics,* **102**(11), doi:10.1002/zamm.202100459 (2022).

[21] G Raghavendra Ganesh, W Sridhar, Khaled Al-Farhany, Sameh E Ahmed. Electrically MHD Casson nanofluid flow and entropy exploration under the influence of the viscous dissipation, radiation, and higher-order chemical reactio, *Physica Scripta*, **97**(6),065208, doi:10.1088/1402-4896/ac6e51 (2022).

[22] G.Dharmaiah, W. Sridhar, K. S. Balamurugan & K. Chandra Kala. Hall and ion slip impact on magneto-titanium alloy nano liquid with diffusion thermo and radiation absorption, *International Journal of Ambient Energy*, **43**(1), 3507–3517, doi:10.1080/01430750.2020.1831597 (2020).

[23] Sridhar, W, Vijaya Lakshmi, G, AL-Farhany, K, Ganesh, GR. MHD Williamson nanofluid across a permeable medium past an extended sheet with constant and irregular thickness. *Heat Transfer*. **50**, 8134- 8154, doi:10.1002/htj.22270 (2021).

[24] Vijaya, N. Arifuzzaman, Raghavendra Sai, Manikya Rao N. Ch. Analysis of Arrhenius Activation Energy in Electrically Conducting Casson Fluid Flow Induced Due to Permeable Elongated Sheet with Chemical Reaction and Viscous Dissipation, *Frontiers in Heat and Mass Transfer (FHMT)* **15**, 1-9, doi:10.5098/hmt.15.26 (2020).

[25] Vijaya, N., Sunil Babu G, Vellanki Lakshmi N., Influence of Critical Parameters on Liquid Thin Film Flow of Casson Nano Fluid Over Elongated Sheet Under Thermophoresis and Brownian Motion, *Frontiers in Heat and Mass Transfer (FHMT)* **15**,1-8, doi:10.5098/hmt.15.23 (2020).

[26] Vijaya, N., Krishna Jyothi, P., Anupama, A., Leelavathi, R., Ambica, K. Thermophoresis and Buoyancy Effects On Chemically Reactive Upper Convected Maxwell Fluid Flow Induced by an Exponentially Stretching Sheet: Application of Cattaneo-Christov Heat Flux, *Frontiers in Heat and Mass Transfer (FHMT)* **17**, 1-8, doi:10.5098/hmt.17.23. (2021).

[27] P. Madhu Sravanthi, M. Radha Madhavi. Nanofluid Flow in Presence of Gyrotactic Microorganisms On the Stretching Surface with Magnetic Field and Activation Energy, *Frontiers in Heat and Mass Transfer (FHMT)*,**19**, 1-9, doi:10.5098/hmt.19.40. (2022).

[28] P. Madhu Sravanthi, M. Radha Madhavi, W.Sridhar. Effects of thermophoresis and chemical reaction on MHD wedge flow of a Casson nanofluid, *AIP Conference Proceedings*,**2707**, 030010. https://doi:10.1063/5.0143366. (2023).

[29] Mardan Ameen Pirdawood, Hemnn Mohammed Rasool, Berivan Faris Aziz. Integrating Sensitivity Analysis and Explicit Runge-Kutta Method for Modeling the Effect of Exposure Rate to Contaminated Water on Cholera Disease Spread. *Passer journal,* **6** (Issue 1) 33-41, doi:10.24271/PSR.2023.412783.1375 (2024).

[30] Garishe Vijaya Lakshmi, Wuriti Sridhar, Saritha Kallu, Srinivasa Rao Thalagadadevi, MHD hybrid nano liquid permeable stretching sheet with radiation heat transfer enhancement effect. *Passer Journal*, Volume 5(Issue 2) 290-297, doi:10.24271/PSR.2023.377379.1201 (2023).

[31] Ali, H.M., Rehman, T.U., Arıcı, M., Said, Z., Duraković, B., Mohammed, H.I., Kumar, R., Rathod, M.K., Buyukdagli, O. and Teggar, M, Advances in thermal energy storage: Fundamentals and Applications. *Progress in Energy and Combustion Science*, **100**, 101109 doi: 10.1016/j.pecs.2023.101109 (2024).